SCIENTIFIC REP🜨RTS

Universal quantum gates for photon-atom hybrid systems assisted by bad cavities

Guan-Yu Wang[1], Qian Liu[1], Hai-Rui Wei[2], Tao Li[3], Qing Ai[1] & Fu-Guo Deng[1]

We present two deterministic schemes for constructing a CNOT gate and a Toffoli gate on photon-atom and photon-atom-atom hybrid quantum systems assisted by bad cavities, respectively. They are achieved by cavity-assisted photon scattering and work in the intermediate coupling region with bad cavities, which relaxes the difficulty of their implementation in experiment. Also, bad cavities are feasible for fast quantum operations and reading out information. Compared with previous works, our schemes do not need any auxiliary qubits and measurements. Moreover, the schematic setups for these gates are simple, especially that for our Toffoli gate as only a quarter wave packet is used to interact the photon with each of the atoms every time. These atom-cavity systems can be used as the quantum nodes in long-distance quantum communication as their relatively long coherence time is suitable for multi-time operations between the photon and the system. Our calculations show that the average fidelities and efficiencies of our two universal hybrid quantum gates are high with current experimental technology.

A quantum computer[1] can run the famous Shor's algorithm[2] for integer factorization and implement Grover-Long algorithm[3,4] for unsorted database search. In past decades, it has attracted much attention. Quantum logic gates are the key elements in quantum computers and play a critical role in quantum information processing (QIP). Two-qubit controlled-not (CNOT) gates together with single-qubit gates are sufficient for universal quantum computing[1,5]. In 2004, Shende proposed a "small-circuit" structure which is used to construct CNOT gates[6]. In the domain of three-qubit gates, Toffoli gate has attracted much attention and it is universal. Together with Hadamard gates, it can realize unitary manipulation for a multi-qubit system[7,8]. Moreover, it plays an important role in phase estimation[1], complex quantum algorithms[2–4], error correction[9], and fault tolerant quantum circuits[10]. In 2009, the optimal synthesis for a Toffoli gate with six CNOT gates was proposed[11]. Up to now, for a general three-qubit logic gate, the optimal synthesis requires twenty CNOT gates[12], which means that this method increases the difficulty and complexity of experiments and the possibility of errors largely. It is significant to seek a simpler scheme to directly implement multi-qubit gates.

By far, many physical systems have been used to implement quantum logic gates, such as photons in the polarization degree of freedom (DOF)[13–15] and those in both the polarization and the spatial-mode DOFs (the hyper-parallel photonic quantum computing)[16–18], nuclear magnetic resonance[19–22], quantum dots[23–27], diamond nitrogen-vacancy center[28–30], superconducting qubits[31,32], superconducting resonators (microwave photons)[33,34], and hybrid quantum systems[35,36]. Cavity quantum electrodynamics (QED) is a promising physical platform for constructing universal quantum logic gates as it can enhance the interaction between a photon and an atom (or an artificial atom). Because of the robustness against decoherence, photons are the perfect candidates for fast and reliable long-distance communication. Meanwhile, the stationary qubits are suitable for processor and local storage. Quantum logic gates between flying photon qubits and stationary qubits hold a great promise for quantum communication and computing, especially for quantum repeaters, distributed quantum computing, and blind quantum computing. Wei and Deng[36] proposed some interesting schemes for universal hybrid quantum gates which use quantum dots inside double-sided optical microcavities as stationary qubits and the flying photon as the control qubit. An atom trapped in an optical microcavity is an attractive candidate for a stationary

[1]Department of Physics, Applied Optics Beijing Area Major Laboratory, Beijing Normal University, Beijing 100875, China. [2]School of Mathematics and Physics, University of Science and Technology Beijing, Beijing 100083, China. [3]State key Laboratory of Low-Dimensional Quantum Physics and Department of Physics, Tsinghua University, Beijing 100084, China. Correspondence and requests for materials should be addressed to F.-G.D. (email: fgdeng@bnu.edu.cn).
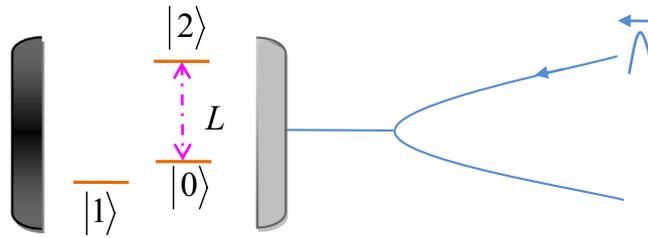
Figure 1. The optical transitions of an atom trapped in a single-sided optical cavity with circularly polarized lights. The *left* wall of the cavity is perfectly reflective and the *right* one is partially reflective. $|0\rangle$, $|1\rangle$, and $|2\rangle$ represent the two ground states and the one excited state of the atom, respectively. L represents the left circularly polarized photon.

qubit. The interaction time between a single atom and the cavity in which the atom is trapped can be maintained for 10 s[37]. By using the atoms interacting with local cavities as the quantum nodes and the photon transmitting between remote nodes as the quantum bus, one can set up a quantum network to realize a large-scale QIP.

Many schemes[38–46] for QIP tasks, assisted by the input-output process in atom-cavity system, have been proposed. Duan and Kimble[41] proposed a scheme for the construction of a controlled phase-flip (CPF) gate between an atom trapped in a cavity and a single photon. The strong coupling between the atom and the cavity can provide a large Kerr nonlinearity. Combined with the input-output process of the flying single photon, a universal quantum gate can be achieved[41]. Interestingly, the atom-photon coupling in a optical cavity have been implemented in experiments. For example, Reiserer *et al.*[47] demonstrated an optical nondestructive detection based on reflecting a photon from an optical cavity[41] containing a single atom in 2013. Tiecke *et al.*[48] realized a system in which a single atom, trapped in a photonic crystal cavity, switches the phase of a photon and a single photon modifies the phase of an atom in 2014. In the same year, Reiserer *et al.*[49] implemented a CPF gate between the spin state of a single trapped atom and the polarization state of a photon. Kalb *et al.*[50] realized a heralded transfer of a polarization qubit from a photon onto a single atom. It is significant for seeking a realization of QIP task in the weak coupling region with a bad cavity. Turchette *et al.*[51] completed a measurement of conditional phase shifts for quantum logic in an intermediate atom-cavity coupling regime with a bad cavity. Dayan *et al.*[52] achieved an experiment in which the transport of photons is regulated by one atom trapped in a cavity in an intermediate atom-cavity coupling regime with a bad cavity. Without the requirements of good cavities or strict strong coupling strength, many theoretical QIP tasks have been proposed, such as quantum gates[53–59], generation of entangled states[60], and quantum controlled teleportation[61]. Xiao *et al.*[53] proposed a scheme of CPF gate without strict strong coupling on a silicon chip. An *et al.*[54] presented a scheme for QIP with a single photon by an input-output process with respect to bad cavities. 2009, Chen *et al.*[55] achieved CPF gates by modifying the original idea proposed by An *et al.*[54].

In this paper, we present a deterministic scheme for constructing a CNOT gate on a hybrid photon-atom system through the atom-cavity photon scattering. In our scheme, the control qubit is encoded on a flying photon (i.e., the two polarization states of a single photon, the right circular polarization and the left circular polarization), while the target qubit is encoded on the ground states of an atom trapped in a bad optical microcavity. We also present a deterministic scheme for constructing a Toffoli gate on a photon-atom-atom hybrid system. We use the atom-cavity systems as our quantum nodes to realize our two quantum gates. The long coherence time of the system is feasible for multi-time operations between the photon and the system and it is suitable for perfect quantum memory. These two gates work in the intermediate coupling region with bad cavities, not require strong coupling strength with good cavities, which relaxes the difficulty of their implementation in experiment. In the bad cavity limit, $\kappa \gg g^2/\kappa \gg \gamma$, it is feasible for fast reading out information, and it is effective for reducing the interaction time between the photon and the atom-cavity system. Our two gates do not require any auxiliary qubits and measurements. Moreover, our schematic setup of the Toffoli gate is very simple, as only a quarter wave packet is used to interact the photon with the atom-cavity system every time, which can reduce the imperfection of the nonlinear interaction. It will be shown that high average fidelities and efficiencies can be achieved for these gates with the intermediate coupling between the atom and the cavity region.

Results

The single-photon input-output process. Let us consider an atom which has two ground states $|0\rangle$ and $|1\rangle$ and an excited state $|2\rangle$ trapped in a single-sided optical cavity, shown in Fig. 1. The cavity considered here is one side wall perfectly reflective and the other side wall partially reflective[41]. The left-circularly L polarized cavity mode couples the transition $|0\rangle \leftrightarrow |2\rangle$ (for example, the D2 transition $(6S_{1/2}, F = 4, m = 4) \rightarrow (6P_{3/2}, F' = 5, m' = 5)$ of cesium), while it decouples the transition $|1\rangle \leftrightarrow |2\rangle$ because of large detuning. Under the Jaynes-Commings model, the Hamiltonian of the whole system composed of a single cavity mode (L polarized) and an atom trapped in a single-sided cavity can be expressed as:

$$H = \frac{\hbar\omega_0}{2}\sigma_z + \hbar\omega_c a^\dagger a + ig\hbar(a\sigma_+ - a^\dagger\sigma_-). \tag{1}$$

Here a and $a^\dagger$ are the annihilation and creation operators of the L polarized cavity mode with the frequency ω_c, respectively. σ_z, σ_+, and σ_- are the inversion, raising, and lowering operators of the atom, respectively. ω_0 is the frequency difference between the ground level $|0\rangle$ and the excited level $|2\rangle$ of the atom. g is the atom-cavity coupling

strength, which is affected by the trapping position of the atom. The reflection coefficient of a single-photon pulse with the frequency ω_p injected into the optical cavity can be obtained by solving the Heisenberg-Langevin equations of motion for the internal cavity field and the atomic operators in the interaction picture[62]:

$$
\begin{aligned}
\dot{a}(t) &= -\left[i(\omega_c - \omega_p) + \frac{\kappa}{2}\right]a(t) - g\sigma_-(t) - \sqrt{\kappa}\,a_{in}(t), \\
\dot{\sigma}_-(t) &= -\left[i(\omega_0 - \omega_p) + \frac{\gamma}{2}\right]\sigma_-(t) - g\sigma_z(t)a(t) + \sqrt{\gamma}\,\sigma_z(t)b_{in}(t), \\
a_{out}(t) &= a_{in}(t) + \sqrt{\kappa}\,a(t).
\end{aligned}
\tag{2}
$$

Here the one-dimensional field operator $a_{in}(t)$ is the cavity input operator which satisfies the commutation relation $[a_{in}(t), a_{in}^\dagger(t')] = \delta(t - t')$. $b_{in}(t)$, with the commutation relation $[b_{in}(t), b_{in}^\dagger(t')] = \delta(t - t')$, is the vacuum input field felt by the three-level atom. a_{out} is the output operator. κ and γ are the cavity damping rate and the atomic decay rate, respectively.

The atom is prepared in the ground states initially. By making κ sufficiently large, one can ensure that the excitation by a single-photon pulse is a weak one, and obtain the input-output relation of the cavity field[54]

$$
r(\omega_p) = \frac{\left[i(\omega_c - \omega_p) - \frac{\kappa}{2}\right]\left[i(\omega_0 - \omega_p) + \frac{\gamma}{2}\right] + g^2}{\left[i(\omega_c - \omega_p) + \frac{\kappa}{2}\right]\left[i(\omega_0 - \omega_p) + \frac{\gamma}{2}\right] + g^2}.
\tag{3}
$$

Here $r(\omega_p) \equiv \frac{a_{out}(t)}{a_{in}(t)}$ is the reflection coefficient for the atom-cavity system. When the atom is uncoupled to the cavity or an empty cavity, that is, $g = 0$, one can obtain[62]

$$
r_0(\omega_p) = \frac{i(\omega_c - \omega_p) - \frac{\kappa}{2}}{i(\omega_c - \omega_p) + \frac{\kappa}{2}}.
\tag{4}
$$

If the atom is initially prepared in the ground state $|0\rangle$, the left-circularly polarized single-photon pulse $|L\rangle$ will drive the transition $|0\rangle \leftrightarrow |2\rangle$. The output pulse related to the input one can be expressed as $|\Phi_{out}\rangle_L = r(\omega_p)|L\rangle \approx e^{i\phi}|L\rangle$. The phase shift ϕ is determined by the parameter values in Eq. (3). However, if the atom is initially prepared in the ground state $|1\rangle$, the left-circularly polarized single-photon $|L\rangle$ will only sense a bare cavity. As a result, the corresponding output governed by Eq. (4) is $|\Phi_{out}\rangle_L = r_0(\omega_p)|L\rangle \approx e^{i\phi_0}|L\rangle$, with a phase shift ϕ_0 different from ϕ. Considering the parameters of the atom-cavity system satisfy the relationship $\omega_0 = \omega_c = \omega_p$, the reflection coefficient can be expressed as

$$
r(\omega_p) = \frac{-1 + (2g/\sqrt{\kappa\gamma})^2}{1 + (2g/\sqrt{\kappa\gamma})^2}, \quad r_0(\omega_p) = -1.
\tag{5}
$$

Considering a bad cavity $\kappa \gg g^2/\kappa \gg \gamma$ in the atom-cavity intermediate coupling region, phase shifts $\phi = 0$ and $\phi_0 = \pi$ from Eq. (5) can be produced.

CNOT gate on a two-qubit hybrid system. Our CNOT gate on a two-qubit hybrid system is used to complete a bit-flip on the atom trapped in the cavity when the flying photon is in the left-circular polarization $|L\rangle$; otherwise, it does nothing. The schematic setup for our CNOT gate is shown in Fig. 2. We will describe its principle in detail as follows.

Suppose that the initial states of the flying photon p and the atom a trapped in the single-sided cavity are

$$
\begin{aligned}
|\psi_p\rangle &= \alpha_p|R\rangle + \beta_p|L\rangle, \\
|\psi_a\rangle &= \alpha|0\rangle + \beta|1\rangle.
\end{aligned}
\tag{6}
$$

First, the flying photon is led to the device shown in Fig. 2. The circularly polarizing beam splitter $CPBS_1$ transmits the photon in the right-circular polarization $|R\rangle$ to path 1 and reflects the photon in the left-circular polarization $|L\rangle$ to path 2. The state of the hybrid system composed of the flying photon p and the atom a is changed from $|\Psi\rangle_0 \equiv |\psi_p\rangle \otimes |\psi_a\rangle$ to $|\Psi\rangle_1$. Here

$$
|\Psi\rangle_1 = \alpha_p|R\rangle_1(\alpha|0\rangle + \beta|1\rangle)_a + \beta_p|L\rangle_2(\alpha|0\rangle + \beta|1\rangle)_a,
\tag{7}
$$

where the subscripts 1 and 2 represent the paths that the flying photon passes through. The subscript a represents the atom trapped in the cavity.

Second, a Hadamard operation is performed on the atom trapped in the cavity before the photon interacts with the atom-cavity system. The Hadamard operation on the atom is used to complete the transformations $|0\rangle \rightarrow \frac{1}{\sqrt{2}}(|0\rangle + |1\rangle)$ and $|1\rangle \rightarrow \frac{1}{\sqrt{2}}(|0\rangle - |1\rangle)$. Thus, the state of the hybrid system is changed to be

$$
\begin{aligned}
|\Psi\rangle_2 = \frac{1}{\sqrt{2}}\{ &\alpha_p|R\rangle_1[\alpha(|0\rangle + |1\rangle) + \beta(|0\rangle - |1\rangle)]_a \\
&+ \beta_p|L\rangle_2[\alpha(|0\rangle + |1\rangle) + \beta(|0\rangle - |1\rangle)]_a\}.
\end{aligned}
\tag{8}
$$
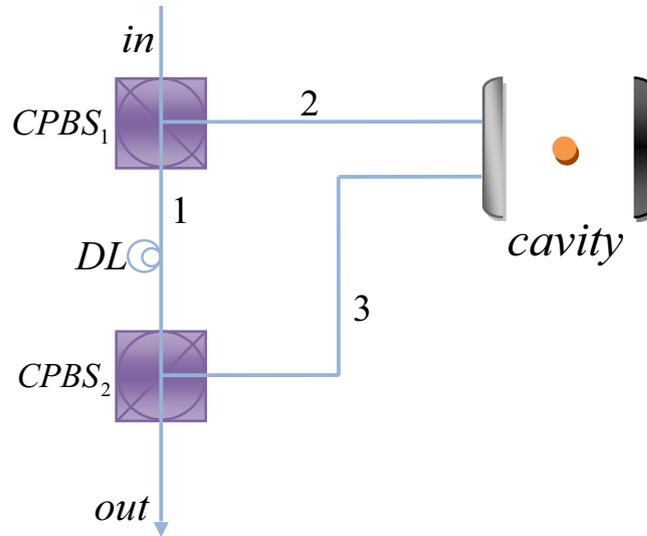
Figure 2. The schematic setup for a deterministic CNOT gate with a flying polarized photon as the control qubit and an atom trapped in a single-sided optical cavity as the target qubit. $CPBS_i$ ($i = 1, 2$) is a circularly polarizing beam splitter which transmits the photon in the right-circular polarization $|R\rangle$ and reflects the photon in the left-circular polarization $|L\rangle$, respectively. M is a mirror. DL is a time-delay device which makes the two wavepackets coming from the paths 2 and 3 interfere with each other.

Third, the photon interacts with the atom trapped in the single-sided cavity and the state of the system becomes

$$|\Psi\rangle_3 = \frac{1}{\sqrt{2}}\{\alpha_p|R\rangle_1[\alpha(|0\rangle + |1\rangle) + \beta(|0\rangle - |1\rangle)]_a$$
$$+ \beta_p|L\rangle_3[\alpha(|0\rangle - |1\rangle) + \beta(|0\rangle + |1\rangle)]_a\}. \tag{9}$$

After the interaction between the flying photon and the atom trapped in the cavity, a Hadamard operation is performed on the atom again. At last, the two wavepacks split by $CPBS_1$ reunion at $CPBS_2$ from path 1 and path 3. The state of the system is transformed into

$$|\Psi\rangle_4 = \alpha_p|R\rangle(\alpha|0\rangle + \beta|1\rangle)_a + \beta_p|L\rangle(\alpha|1\rangle + \beta|0\rangle)_a. \tag{10}$$

Here $|\Psi\rangle_4$ is the objective state. One can see that the state of the atom (the target qubit) is flipped when the photon (the control qubit) is in the left-circular polarization $|L\rangle$; otherwise, nothing is done on the atom. That is, the schematic setup shown in Fig. 2 can be used to deterministically achieve a quantum CNOT gate on the photon-atom hybrid system by using the flying photon as the control qubit and the atom as the target qubit in principle.

Toffoli gate on a three-qubit hybrid system. Our Toffoli gate on a three-qubit hybrid system is used to complete a bit-flip operation on the atom trapped in $cavity2$ (the target qubit) when the polarization of the flying photon (the first control qubit) is in the left-circular polarization $|L\rangle$ and the atom trapped in $cavity1$ (the second control qubit) is in the state $|1\rangle$ at the same time; otherwise, it does nothing on the atom trapped in $cavity2$. The schematic setup of our Toffoli gate is shown in Fig. 3. Assume that the initial states of the flying photon qubit and the two atoms trapped in $cavity$ 1 and $cavity$ 2 are prepared in $|\phi_p\rangle$, $|\phi_{a1}\rangle$, and $|\phi_{a2}\rangle$, respectively. Here,

$$|\phi_p\rangle = \alpha_p|R\rangle + \beta_p|L\rangle,$$
$$|\phi_{a1}\rangle = \alpha_1|0\rangle + \beta_1|1\rangle,$$
$$|\phi_{a2}\rangle = \alpha_2|0\rangle + \beta_2|1\rangle. \tag{11}$$

The principle of our Toffoli gate can be described in detail as follows.

First, the photon is led into our device from the port in. $CPBS_1$ reflects the photon in the left-circular polarization $|L\rangle$ to path 1 and transmits the photon in the right-circular polarization $|R\rangle$ to path 2. The photon passing through path 2 will not interact with the atoms trapped in cavities. After the photon passes through $CPBS_1$, the state of the system is changed from $|\Phi\rangle_0 \equiv |\phi_p\rangle \otimes |\phi_{a1}\rangle \otimes |\phi_{a2}\rangle$ to $|\Phi\rangle_1$. Here,

$$|\Phi\rangle_1 = \alpha_p|R\rangle_2 \otimes (\alpha_1|0\rangle + \beta_1|1\rangle)_{a_1} \otimes (\alpha_2|0\rangle + \beta_2|1\rangle)_{a_2}$$
$$+ \beta_p|L\rangle_1 \otimes (\alpha_1|0\rangle + \beta_1|1\rangle)_{a_1} \otimes (\alpha_2|0\rangle + \beta_2|1\rangle)_{a_2}. \tag{12}$$
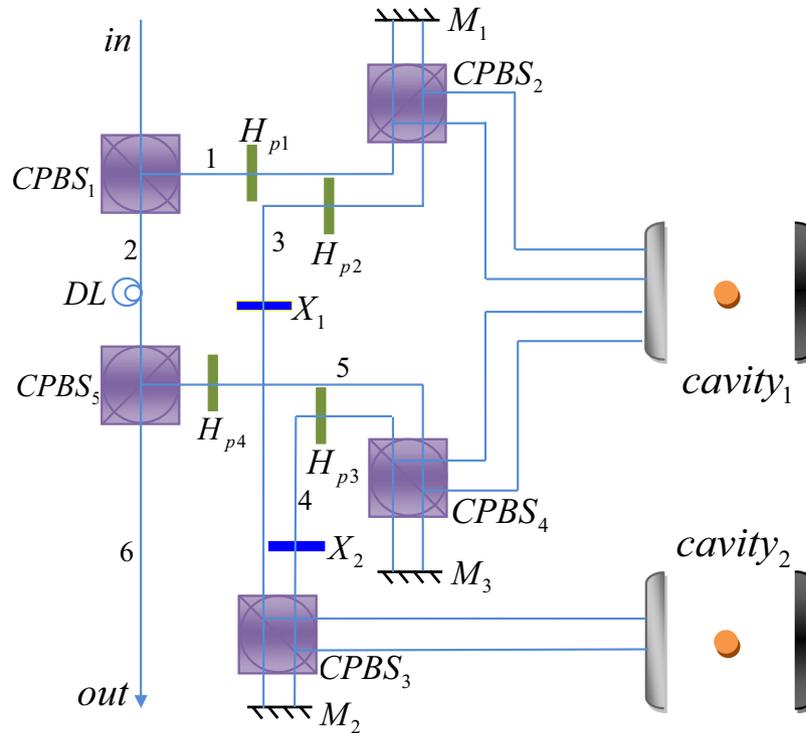
Figure 3. The schematic setup for constructing a deterministic Toffoli gate with the polarization of a flying photon and an atom trapped in a single-sided cavity ($cavity_1$) as the two control qubits and anther atom trapped in another single-sided cavity ($cavity_2$) as the target qubit. $H_{pi} (i = 1, 2, 3, 4)$ is a half-wave plate with the axis at 22.5° and it performs a Hadamard operation on the photon. X_i ($i = 1, 2$) represents a half-wave plate which performs a bit-flip operation on the photon. M_i ($i = 1, 2, 3$) is a mirror. $cavity_i$ ($i = 1, 2$) represents the atom-cavity system.

Second, a Hadamard operation is performed on the photon in path 1, and $CPBS_2$ transmits the photon in $|R\rangle$ to M_1 and reflects the photon in $|L\rangle$ to $cavity$ 1. Here the Hadamard operation on the photon completes the transformations $|R\rangle \rightarrow \frac{1}{\sqrt{2}}(|R\rangle + |L\rangle)$ and $|L\rangle \rightarrow \frac{1}{\sqrt{2}}(|R\rangle - |L\rangle)$. Subsequently, the flying photon interacts with the atom trapped in $cavity$ 1. After the interaction, the two components of the photon reunion at $CPBS2$. Also, a Hadamard operation and a bit-flip operation $\sigma_x = |L\rangle\langle R| + |R\rangle\langle L|$ are performed on the photon in path 3. The state of the whole system becomes

$$\begin{aligned}
|\Phi\rangle_2 &= \alpha_p |R\rangle_2 (\alpha_1 |0\rangle + \beta_1 |1\rangle)_{a_1} \otimes (\alpha_2 |0\rangle + \beta_2 |1\rangle)_{a_2} + \beta_p |R\rangle_3 \alpha_1 |0\rangle_{a1} \\
&\otimes (\alpha_2 |0\rangle + \beta_2 |1\rangle)_{a_2} + \beta_p |L\rangle_3 \beta_1 |1\rangle_{a1} \otimes (\alpha_2 |0\rangle + \beta_2 |1\rangle)_{a_2}.
\end{aligned} \tag{13}$$

Third, one can perform a Hadamard operation on the atom trapped in $cavity$ 2 and lead the photon in $|L\rangle$ reflected by $CPBS_3$ to $cavity$ 2 and the photon in $|R\rangle$ transmitted by $CPBS_3$ to M_2. The photon in $|L\rangle$ and the atom trapped in $cavity$ 2 interact with each other. After the interaction, a Hadamard operation is performed on the atom trapped in $cavity$ 2 again. The two components of the photon reunion at $CPBS_3$. The state of the whole system is changed into

$$\begin{aligned}
|\Phi\rangle_3 &= \alpha_p |R\rangle_2 (\alpha_1 |0\rangle + \beta_1 |1\rangle)_{a_1} \otimes (\alpha_2 |0\rangle + \beta_2 |1\rangle)_{a_2} \\
&+ \beta_p |R\rangle_4 \alpha_1 |0\rangle_{a1} (\alpha_2 |0\rangle + \beta_2 |1\rangle)_{a_2} + \beta_p |L\rangle_4 \beta_1 |1\rangle_{a1} (\alpha_2 |1\rangle + \beta_2 |0\rangle)_{a_2}.
\end{aligned} \tag{14}$$

Finally, a bit-flip operation and a Hadamard operation are performed on the photon which emerges in path 4. $CPBS_4$ transmits the photon in $|R\rangle$ to M_3 and reflects the photon in $|L\rangle$ to $cavity$ 1. The photon in $|L\rangle$ interacts with the atom trapped in $cavity$ 1 again. After the interaction between the atom-cavity system and the photon, $CPBS_4$ reflects the photon in $|L\rangle$ and transmits the photon in $|R\rangle$ to path 5. The former is reflected by $cavity$ 1 and the latter is reflected by M_3. A Hadamard operation is performed on the photon in path 5. At this time, the two components of the photon from paths 2 and 5 pass through $CPBS_5$ simultaneously, and then the photon is led out of our device. The final state of the whole system composed of the flying photon and the two atoms trapped in two cavities separately can be expressed as

$$
\begin{aligned}
|\Phi\rangle_f \;=\; & \alpha_p|R\rangle\alpha_1|0\rangle_{a_1}(\alpha_2|0\rangle + \beta_2|1\rangle)_{a_2} + \beta_p|L\rangle\alpha_1|0\rangle_{a_1}(\alpha_2|0\rangle + \beta_2|1\rangle)_{a_2} \\
& + \alpha_p|R\rangle\beta_1|1\rangle_{a_1}(\alpha_2|0\rangle + \beta_2|1\rangle)_{a_2} + \beta_p|L\rangle\beta_1|1\rangle_{a_1}(\alpha_2|1\rangle + \beta_2|0\rangle)_{a_2}.
\end{aligned}
\tag{15}
$$

From Eq. (15), one can see that the state of the atom trapped in *cavity* 2 (the target qubit) is flipped only when the photon (the first control qubit) is in the left-circular polarization $|L\rangle$ and the atom trapped in *cavity* 1 (the second control qubit) is in $|1\rangle$ at the same time. That is, the schematic setup shown in Fig. 3 can achieve a quantum Toffoli gate on a photon-atom-atom hybrid system by using the flying photon and the atom in *cavity* 1 as the two control qubits and the atom in *cavity* 2 as the target qubit in a deterministic way.

Discussion

Reiserer *et al.*[47] exploited the atom-cavity system to complete a robust photon detection scheme experimentally. In their experiment, a single ^{87}Rb atom is trapped at the center of a Fabry-Perot resonator[63]. Their experiment was completed in the experimental parameters $[g, \kappa, \gamma]/2\pi = [6.7, 2.5, 3.0]MHz$. In the same experimental parameters, they[49] implemented a quantum CNOT gate that a flip of the photon is controlled by an atom trapped in a Fabry-Perot cavity. Tiecke *et al.*[48] realized a scheme in which a single atom switches the phase of a photon and a single photon modifies the atom's phase. Their experiment was implemented in the parameters $[2g, \kappa, \gamma]/2\pi = [(1.09 \pm 0.03)\,GHz, 25\,GHz, 6\,MHz]$. Compared with intermediate coupling strength of the atom-cavity system, it is still challenging to realize the strong coupling strength in experiment. For obtaining shorter operation time, it is significant to realize the atom-cavity photon scattering with a bad cavity in experiment. Turchette *et al.*[51] made a measurement on the conditional phase shifts for quantum logic in the experimental parameters $[g, \kappa, \gamma]/2\pi = [20, 75, 2.5]MHz$. These parameters satisfy the limit of a bad cavity $\kappa \gg g^2/\kappa \gg \gamma$ and an intermediate coupling region ($g = 0.27\kappa$). Based on these experimental parameters, the average fidelities of our CNOT gate and Toffoli gate are $\overline{F}_C = 0.9943$ and $\overline{F}_T = 0.9885$, respectively. The average efficiencies of our CNOT gate and Toffoli gate are $\overline{P}_C = 0.9061$ and $\overline{P}_T = 0.8631$, respectively. Dayan *et al.*[52] demonstrated an intermediate atom-cavity coupling in experiment. In their experiment, a Cs atom is trapped in a microtoroidal resonator. They gave a set of parameters $[g, \kappa, \gamma]/2\pi = [70, (165 \pm 15), 2.6]MHz$. The probe laser can be swept continuously over a range $\Delta = \omega_p - \omega_c = \pm 400$ MHz and the atom-cavity detuning $\omega_0 - \omega_c = 0$ can be obtained. The parameters in their experiment satisfy the requirements of a bad cavity and an intermediate coupling regime ($g = 0.38\kappa$). Based on these experimental parameters, the average fidelities of our CNOT gate and Toffoli gate are $\overline{F}_C = 0.9998$ and $\overline{F}_T = 0.9994$, respectively. The average efficiencies of our CNOT gate and Toffoli gate are $\overline{P}_C = 0.9772$ and $\overline{P}_T = 0.9661$, respectively. The analyses above show that the average fidelities and the averages efficiencies of our two gates can remain high values in the intermediate coupling region with a bad cavity.

In contrary to the CNOT scheme presented by Bonant *et al.*[35], in which a confined electron spin in a QD trapped in a cavity acts as a control qubit and the spin of the photon acts as a target qubit, we use a flying photon as a control qubit and use an atom trapped in an cavity as a target qubit. Our scheme is different from the CNOT scheme proposed by Reiserer *et al.*[49], in which an atom trapped in a cavity acts as a control qubit and the polarization state of the photon acts as a target qubit. In our scheme, the two different polarizations of the photon are split by the CPBS before the photon interacts with the atom-cavity system, which will reduce the difficulty of the experiment. Our scheme is also different from the work by Su *et al.*[59] in which an atom trapped in an cavity acts as the control qubit and an atom trapped in another cavity acts as the target qubit with an auxiliary atom qubit and measurements on the auxiliary qubit and the photon.

In summary, we have proposed two schemes for constructing a deterministic CNOT gate and a deterministic Toffoli gate on photon-atom hybrid systems, respectively, by utilizing the nonlinear interaction between the flying photon and the atom-cavity system and some linear optical elements. For our CNOT gate, the control qubit is encoded on the flying photon and the target qubit is encoded on the atom trapped in the cavity. For our Toffoli gate, the control qubits are encoded on the flying photon and an atom trapped in one cavity and the target qubit is encoded on an atom trapped in another cavity. The quantum circuits of our two gates are very simple. They do not need any auxiliary qubit and measurements to complete the CNOT and Toffoli gates on photon-atom hybrid systems. Our two schemes can work in the atom-cavity intermediate coupling region with bad cavities. The atom-cavity system working in the intermediate coupling region is achieved in experiment[51,52]. The ratio of coupling strength to dissipation factors $g/\sqrt{\kappa\gamma}$ affects the fidelities and efficiencies of our gates a little. Our calculations show that even in a worst condition or a reasonable experimental condition, the average of fidelities and the average efficiencies of our two gates can remain high values. What's more, there exist experimental parameters that satisfy the requirements in this work.

Methods

Fidelities and efficiencies of the gates. The nonlinear interaction between the single photon and the atom-cavity system produces a phase shift between the output photon and the input photon. Utilizing this shift and some linear optical elements we construct a CNOT gate and a Toffoli gate on photon-atom and photon-atom-atom hybrid quantum systems, respectively. In the process of constructing these two universal quantum hybrid gates, we set $\phi_0 = \pi$ and $\phi = 0$. In this ideal case, the hybrid quantum gates are deterministic, and the fidelity and the efficiency are 100% for each gate. However, the phase shift $\phi_0 = \pi$ is an exact value when $g = 0$, while the phase shift $\phi = 0$ is an approximate value when $\kappa \gg g^2/\kappa \gg \gamma$. It is a function of $g/\sqrt{\kappa\gamma}$, which is decided by the experimental condition. Considering the realistic condition, we will calculate the fidelities of our quantum gates to show their performance. The fidelity is defined as $F = |\langle\Psi_r|\Psi_i\rangle|^2$. Here $|\Psi_r\rangle$ and $|\Psi_i\rangle$ are final states of the hybrid quantum system in our schemes for quantum gates in the realistic condition and the ideal condition, respectively.
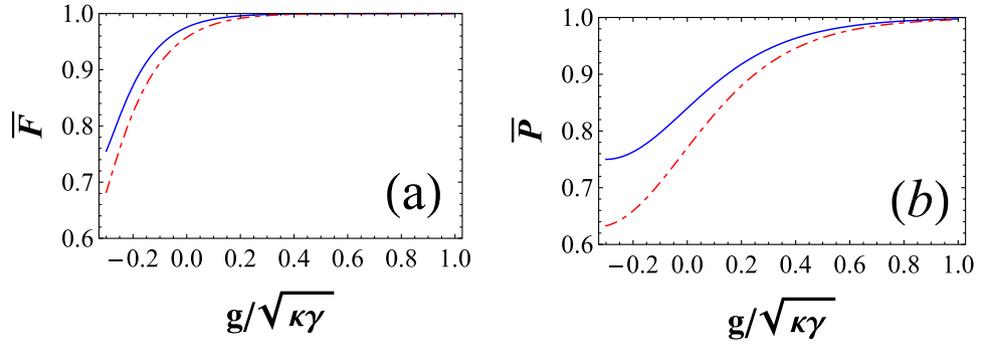
Figure 4. (**a**) Average fidelity $\overline{F}$ of our CNOT gate on a two-qubit hybrid system (solid line) and that of our Toffoli gate on a three-qubit hybrid system (dashed line) vs $g/\sqrt{\kappa\gamma}$ on a logarithmic scale. (**b**) Average efficiency $\overline{P}$ of our CNOT gate on a two-qubit hybrid system (solid line) and that of our Toffoli gate on a three-qubit hybrid system (dashed line) vs $g/\sqrt{\kappa\gamma}$ on a logarithmic scale.

The fidelity of our CNOT gate is expressed as

$$F_C = \frac{\left|\alpha_p^2 + \frac{1}{2}\beta_p^2[2\alpha\beta(r-1) + r + 1]\right|^2}{\left|\alpha_p\right|^2 + \frac{1}{4}\left|\alpha\beta_p(r-1) + \beta\beta_p(r+1)\right|^2 + \frac{1}{4}\left|\alpha\beta_p(r+1) + \beta\beta_p(r-1)\right|^2}. \tag{16}$$

The coefficients of the system can be expressed as $\alpha_p = \cos\varphi$, $\beta_p = \sin\varphi$, $\alpha = \cos\theta$, and $\beta = \sin\theta$. The average fidelity of the CNOT gate is

$$\overline{F}_C = \frac{1}{4\pi^2}\int_0^{2\pi}\int_0^{2\pi} F_C d\varphi\,d\theta. \tag{17}$$

The relationship between the average fidelity of our CNOT gate and $g/\sqrt{\kappa\gamma}$ on a logarithmic scale is shown in Fig. 4(a) with the solid line. For our Toffoli gate on a three-qubit hybrid system, its fidelity is

$$F_T = \frac{\left|\alpha_p^2 + \frac{\beta_p^2\alpha_1^2}{8}[(r-1)^3 + 2\alpha_2\beta_2(r-1)^2(r+1) + 2(r+1)^2] + \frac{\beta_p^2\beta_1^2}{2}[2\alpha_2\beta_2(r-1) + r + 1]\right|^2}{\xi_1 + \xi_2 + \xi_3 + \xi_4 + \xi_5 + \xi_6}. \tag{18}$$

Here $\xi_1 = |\alpha_p|^2$, $\xi_2 = \frac{1}{64}|\beta_p\alpha_1[\alpha_2(r-1)^3 + \beta_2(r-1)^2(r+1) + 2\alpha_2(r+1)^2]|^2$, $\xi_3 = \frac{1}{64}|\beta_p\alpha_1[\beta_2(r-1)^3 + \alpha_2(r-1)^2(r+1) + 2\beta_2(r+1)^2]|^2$, $\xi_4 = \frac{1}{4}|\beta_p\beta_1[\alpha_2(r-1) + \beta_2(r+1)]|^2$, $\xi_5 = \frac{1}{4}|\beta_p\beta_1[\alpha_2(r+1) + \beta_2(r-1)]|^2$, and $\xi_6 = \frac{1}{32}|\beta_p\alpha_1[\alpha_2(1+r)^2(1-r) + \beta_2(1+r)^2(1-r)]|^2$. The coefficients of the system can be expressed as $\alpha_p = \cos\varphi$, $\beta_p = \sin\varphi$, $\alpha_1 = \cos\theta$, $\beta_1 = \sin\theta$, $\alpha_2 = \cos\eta$, and $\beta_2 = \sin\eta$. The average fidelity of our Toffoli gate is

$$\overline{F}_T = \frac{1}{8\pi^3}\int_0^{2\pi}\int_0^{2\pi}\int_0^{2\pi} F_T d\varphi d\theta d\eta. \tag{19}$$

The dashed line in Fig. 4(a) shows the relationship between the average fidelity of our Toffoli gate and $g/\sqrt{\kappa\gamma}$ on a logarithmic scale.

The efficiency of a quantum gate is defined as $P = \frac{n_{out}}{n_{in}}$, where n_{out} is the number of the photons coming out of the device and n_{in} is the number of the photons led into the device. The efficiency of our CNOT gate is

$$P_C = \left|\alpha_p\right|^2 + \frac{1}{4}\left|\alpha\beta_p(r-1) + \beta\beta_p(r+1)\right|^2 + \frac{1}{4}\left|\alpha\beta_p(r+1) + \beta\beta_p(r-1)\right|^2. \tag{20}$$

The average efficiency of our CNOT gate is

$$\overline{P}_C = \frac{1}{4\pi^2}\int_0^{2\pi}\int_0^{2\pi} P_C d\varphi d\theta. \tag{21}$$

The relationship between the average efficiency of our CNOT gate and $g/\sqrt{\kappa\gamma}$ on a logarithmic scale is shown in Fig. 4(b) with the solid line.

The efficiency of our Toffoli gate is

$$P_T = \xi_1 + \xi_2 + \xi_3 + \xi_4 + \xi_5. \tag{22}$$

We can also calculate the average efficiency of our Toffoli gate

$$\overline{P}_T = \frac{1}{8\pi^3} \int_0^{2\pi} \int_0^{2\pi} \int_0^{2\pi} P_T d\varphi d\theta d\eta. \tag{23}$$

The dashed line in Fig. 4(b) shows the relationship between the average efficiency of our Toffoli gate and $g/\sqrt{\kappa\gamma}$ on logarithmic scale. From Fig. 4(a,b), one can see that the average fidelities and average efficiencies of these two universal quantum gates are affected by the cooperativity C ($\propto g/\sqrt{\kappa\gamma}$) of the atom-cavity system. The average fidelities are relatively sensitive to the cooperativity when $g/\sqrt{\kappa\gamma} < 1$ (0 on a logarithmic scale) and they are faintly affected by cooperativity when $g/\sqrt{\kappa\gamma} > 1.5$ (0.17 on a logarithmic scale). If $g/\sqrt{\kappa\gamma} \geq 1.5$, which is not a difficult experimental requirement, the average fidelities of our CNOT and Toffoli gates can be higher than 0.9949 and 0.9896, respectively. The average efficiencies are relatively sensitive to the cooperativity when $g/\sqrt{\kappa\gamma} < 2$ (0.3 on a logarithmic scale) and they are faintly affected by the cooperativity when $g/\sqrt{\kappa\gamma} > 3$ (0.48 on a logarithmic scale). If $g/\sqrt{\kappa\gamma} \geq 3$, which is not a difficult experimental requirement, the average efficiencies of our CNOT and Toffoli gates can be higher than 0.9737 and 0.9609, respectively.

Except for the cooperativity C, some other realistic losses and imperfections, that would affect the fidelities and the efficiencies of our schemes, should be taken into account. The mismatching of spatial mode between cavity and the input photon, the quality of atomic state preparation and rotation will affect both of the fidelities and the efficiencies of our schemes[49]. The fidelities of our schemes will be also affected by the small probability of more than one photon in the input laser pulses[49]. The efficiencies can be also affected by the stability of difference between the cavity resonance and the frequency of the input photon and the imperfect absorption losses of the mirror of the cavity[49]. In our scheme, as only one polarization of a photon is injected to the atom-cavity system and the two polarizations are split by the *CPBS*, the precise timing of the arrival times from different photon paths is required in the realistic experiment.

References

1. Nielsen, M. A. & Chuang, I. L. *Quantum Computation and Quantum Information* (Cambridge University, Cambridge, 2000).
2. Shor, P. W. Polynomial-time algorithms for prime factorization and discrete logarithms on a quantum computer. *SIAM J. Comput.* **26,** 1484–1509 (1997).
3. Grover, L. K. Quantum mechanics helps in searching for a needle in a haystack. *Phys. Rev. Lett.* **79,** 325 (1997).
4. Long, G. L. Grover algorithm with zero theoretical failure rate. *Phys. Rev. A* **64,** 022307 (2001).
5. Barenco, A. *et al.* Elementary gates for quantum computation. *Phys. Rev. A* **52,** 3457–3467 (1995).
6. Shende, V. V., Bullock, S. S. & Markov, I. L. Recognizing small-circuit structure in two-qubit operators. *Phys. Rev. A* **70,** 012310 (2005).
7. Shi, Y. Y. Both Toffoli and controlled-NOT need little help to do universal quantum computing. *Quant. Inf. Comput.* **3,** 84–92 (2003).
8. Fredkin, E. & Toffoli, T. Conservative logic. *Int. J. Theor. Phys.* **21,** 219–253 (1982).
9. Cory, D. G. *et al.* Experimental quantum error correction. *Phys. Rev. Lett.* **81,** 2152–2155 (1998).
10. Dennis, E. Toward fault-tolerant quantum computation without concatenation. *Phys. Rev. A* **63,** 052314 (2001).
11. Shende, V. V. & Markov, I. L. On the CNOT-cost of Toffoli gates. *Quant. Inf. Comput.* **9,** 461–486 (2009).
12. Shende, V. V., Bullock, S. S. & Markov, I. L. Synthesis of quantum-logic circuits. *IEEE Trans. on Computer-Aided Design* **25,** 1000–1010 (2006).
13. Knill, E., Laflamme, R. & Milburn, G. J. A scheme for efficient quantum computation with linear optics. *Nature* **409,** 46–52 (2001).
14. O'Brien, J. L., Pryde, G. J., White, A. G., Ralph, T. C. & Branning, D. Demonstration of an all-optical quantum controlled-NOT gate. *Nature* **426,** 264–267 (2003).
15. Wei, H. R. & Deng, F. G. Scalable photonic quantum computing assisted by quantum-dot spin in double-sided optical microcavity. *Opt. Express* **21,** 17671–17685 (2013).
16. Ren, B. C., Wei, H. R. & Deng, F. G. Deterministic photonic spatial-polarization hyper-controlled-not gate assisted by a quantum dot inside a one-side optical microcavity. *Laser Phys. Lett.* **10,** 095202 (2013).
17. Ren, B. C. & Deng, F. G. Hyper-parallel photonic quantum computation with coupled quantum dots. *Sci. Rep.* **4,** 4623 (2014).
18. Ren, B. C., Wang, G. Y. & Deng, F. G. Universal hyperparallel hybrid photonic quantum gates with dipole-induced transparency in the weak-coupling regime. *Phys. Rev. A* **91,** 032328 (2015).
19. Gershenfeld, N. A. & Chuang, I. L. Bulk spin-resonance quantum computation. *Science* **275,** 350–356 (1997).
20. Jones, J. A., Mosca, M. & Hansen, R. H. Implementation of a quantum search algorithm on a quantum computer. *Nature* **393,** 344–346 (1998).
21. Long, G. L. & Xiao, L. Experimental realization of a fetching algorithm in a 7-qubit NMR spin Liouville space computer. *J. Chem. Phys.* **119,** 8473–8481 (2003).
22. Feng, G. R., Xu, G. F. & Long, G. L. Experimental realization of nonadiabatic holonomic quantum computation. *Phys. Rev. Lett.* **110,** 190501 (2013).
23. Li, X. Q. *et al.* An all-optical quantum gate in a semiconductor quantum dot. *Science* **301,** 809–811 (2003).
24. Hu, C. Y., Young, A., O'Brien, J. L., Munro, W. J. & Rarity, J. G. Giant optical Faraday rotation induced by a single-electron spin in a quantum dot: applications to entangling remote spins via a single photon. *Phys. Rev. B* **78,** 085307 (2008).
25. Hu, C. Y., Munro, W. J. & Rarity, J. G. Deterministic photon entangler using a charged quantum dot inside a microcavity. *Phys. Rev. B* **78,** 125318 (2008).
26. Wei, H. R. & Deng, F. G. Universal quantum gates on electron-spin qubits with quantum dots inside single-side optical microcavities. *Opt. Express* **22,** 593–607 (2014).
27. Wang, H. F., Zhu, A. D., Zhang, S. & Yeon, K. H. Optically controlled phase gate and teleportation of a controlled-NOT gate for spin qubits in a quantum-dot-microcavity coupled system. *Phys. Rev. A* **87,** 062337 (2013).
28. Togan, E. *et al.* Quantum entanglement between an optical photon and a solid-state spin qubit. *Nature* **466,** 730–734 (2010).
29. Wei, H. R. & Deng, F. G. Compact quantum gates on electron-spin qubits assisted by diamond nitrogen-vacancy centers inside cavities. *Phys. Rev. A* **88,** 042323 (2013).
30. Neumann, P. *et al.* Quantum register based on coupled electron spins in a room-temperature solid. *Nat. Phys.* **6,** 249–253 (2010).
31. Yamamoto, T., Pashkin, Y. A., Astafiev, O., Nakamura, Y. & Tsai, J. S. Demonstration of conditional gate operation using superconducting charge qubits. *Nature* **425,** 941–944 (2003).
32. Clarke, J. & Wilhelm, F. K. Superconducting quantum bits. *Nature* **453,** 1031–1042 (2008).

33. Hua, M., Tao, M. J. & Deng, F. G. Fast universal quantum gates on microwave photons with all-resonance operations in circuit QED. *Sci. Rep.* **5,** 9274 (2015).
34. Hua, M., Tao, M. J. & Deng, F. G. Universal quantum gates on microwave photons assisted by circuit quantum electrodynamics. *Phys. Rev. A* **90,** 012328 (2014).
35. Bonato, C. *et al.* CNOT and Bell-state analysis in the weak-coupling cavity QED regime. *Phys. Rev. Lett.* **104,** 160503 (2010).
36. Wei, H. R. & Deng, F. G. Universal quantum gates for hybrid systems assisted by quantum dots inside double-sided optical microcavities. *Phys. Rev. A* **87,** 022305 (2013).
37. Fortier, K. M., Kim, Y., Gibbons, M. J., Ahmadi, P. & Chapman, M. S. Deterministic loading of individual atoms to a high-finesse optical cavity. *Phys. Rev. Lett.* **98,** 233601 (2007).
38. Cirac, J. I., Zoller, P., Kimble, H. J. & Mabuchi, H. Quantum state transfer and entanglement distribution among distant nodes in a quantum network. *Phys. Rev. Lett.* **78,** 3221–3224 (1997).
39. Boozer, A. D., Boca, A., Miller, R., Northup, T. E. & Kimble, H. J. Reversible state transfer between light and a single trapped atom. *Phys. Rev. Lett.* **98,** 193601 (2007).
40. Duan, L. M., Kuzmich, A. & Kimble, H. J. Cavity QED and quantum-information processing with "hot" trapped atoms. *Phys. Rev. A* **67,** 032305 (2003).
41. Duan, L. M. & Kimble, H. J. Scalable photonic quantum computation through cavity-assisted interactions. *Phys. Rev. Lett.* **92,** 127902 (2004).
42. Duan, L. M., Wang, B. & Kimble, H. J. Robust quantum gates on neutral atoms with cavity-assisted photon scattering. *Phys. Rev. A* **72,** 032333 (2005).
43. Cho, J. Y. & Lee, H. W. Generation of atomic cluster states through the cavity input-output process. *Phys. Rev. Lett.* **95,** 160501 (2005).
44. Liang, L. M. & Li, C. Z. Realization of quantum SWAP gate between flying and stationary qubits. *Phys. Rev. A* **72,** 024303 (2005).
45. Wang, B. & Duan, L. M. Implementation scheme of controlled SWAP gates for quantum fingerprinting and photonic quantum computation. *Phys. Rev. A* **75,** 050304(R) (2007).
46. Lin, X. M., Xue, P., Chen, M. Y., Chen, Z. H. & Li, X. H. Scalable preparation of multiple-particle entangled states via the cavity input-output process. *Phys. Rev. A* **74,** 052339 (2006).
47. Reiserer, A., Ritter, S. & Rempe, G. Nondestructive detection of an optical photon. *Science* **342,** 1349 (2013).
48. Tiecke, T. G. *et al.* Nanophotonic quantum phase switch with a single atom. *Nature* **508,** 241–244 (2014).
49. Reiserer, A., Kalb, N., Rempe, G. & Ritter, S. A quantum gate between a flying optical photon and a single trapped atom. *Nature* **508,** 237–240 (2014).
50. Kalb, N., Reiserer, A., Ritter S. & Rempe, G. Heralded storage of a photonic quantum bit in a single atom. *Phys. Rev. Lett.* **114,** 220501 (2015).
51. Turchette, Q. A., Hood, C. J., Lange, W., Mabuchi, H. & Kimble, H. J. Measurement of conditional phase shifts for quantum logic. *Phys. Rev. Lett.* **75,** 4710–4713 (1995).
52. Dayan, B. *et al.* A photon turnstile dynamically regulated by one atom. *Science* **319,** 1062 (2008).
53. Xiao, Y. F., Han, Z. F. & Guo G. C. Quantum computation without strict strong coupling on a silicon chip. *Phys. Rev. A* **73,** 052324 (2006).
54. An, J. H., Feng, M. & Oh, C. H. Quantum-information processing with a single photon by an input-output process with respect to low-Q cavities. *Phys. Rev. A* **79,** 032303 (2009).
55. Chen, Q. & Feng, M. Quantum gating on neutral atoms in low-Q cavities by a single-photon input-output process. *Phys. Rev. A* **79,** 064304 (2009).
56. Song, J., Xia, Y. & Song, H. S. Quantum gate operations using atomic qubits through cavity input-output process. *Eur. Phys. Lett.* **87,** 50005 (2009).
57. Bastos, W. P., Cardoso, W. B., Avelar, A. T. & Baseia, B. A note on entanglement swapping of atomic states through the photonic Faraday rotation. *Quant. Inf. Process.* **10,** 395–404 (2011).
58. Mei, F., Yu, Y. F., Feng, X. L., Zhu, S. L. & Zhang, Z. M. Optical quantum computation with cavities in the intermediate coupling region. *Eur. Phys. Lett.* **91,** 10001 (2010).
59. Su, S. L., Guo, Q., Zhu, L., Wang, H. F. & Zhang, S. Atomic quantum information processing in low-Q cavity in the intermediate coupling region. *J. Opt. Soc. Am. B* **29,** 2827–2833 (2012).
60. Mei, F., Feng, M., Yu, Y. F. & Zhang, Z. M. Scalable quantum information processing with atomic ensembles and flying photons. *Phys. Rev. A* **80,** 042319 (2009).
61. Bastos, W. P., Cardoso, W. B., Avelar, A. T., de Almeida, N. G. & Baseia, B. Controlled teleportation via photonic Faraday rotations in low-Q cavities. *Quant. Inf. Process.* **11,** 1867 (2012).
62. Walls, D. F. & Milburn, G. J. *Quantum optics* (Springer-Verlag, Berlin, 1994).
63. Reiserer, A., Nölleke, C., Ritter, S. & Rempe, G. Ground-state cooling of a single atom at the center of an optical cavity. *Phys. Rev. Lett.* **110,** 223003 (2013).

Acknowledgements

Author Contributions

G.-Y.W., Q.L., H.-R.W., Q.A. and F.-G.D. wrote the main manuscript text, and prepared Figures 1–5. G.-Y.W., H.-R.W., T.L. and F.-G.D. did the calculations. F.-G.D. supervised the whole project. All authors reviewed the manuscript.

Additional Information

Competing financial interests: The authors declare no competing financial interests.

How to cite this article: Wang, G.-Y. *et al.* Universal quantum gates for photon-atom hybrid systems assisted by bad cavities. *Sci. Rep.* **6**, 24183; doi: 10.1038/srep24183 (2016).